

## Preparation of Dialdehyde Chitosan and its Application in Green Synthesis of Silver Nanoparticles

Yong Lv,<sup>a,b</sup> Zhu Long,<sup>a,\*</sup> Ci Song,<sup>b</sup> Lei Dai,<sup>a</sup> Hong He,<sup>a</sup> and Ping Wang<sup>a</sup>

A simple, green method was developed for the synthesis of silver nanoparticles (AgNPs) by using Dialdehyde Chitosan (D-CTS) as the reducing and stabilizing agent. D-CTS was prepared from the oxidation of chitosan by sodium periodate, and its degree of oxidation was determined by <sup>1</sup>H-NMR and elemental analysis. The synthesized AgNPs were characterized by UV-Vis spectroscopy, dynamic light scattering (DLS), Fourier-transform infrared spectroscopy (FT-IR), X-ray diffraction (XRD), and scanning electron microscopy (SEM). The morphology and size distribution of the AgNPs were found to vary with the dialdehyde content of D-CTS and the pH value of the reaction solution. FT-IR spectra revealed that the aldehyde groups and the amino groups were the major agents that stabilized the AgNPs. XRD results indicated the presence of nano-silver having a face-centered cubic structure. SEM results showed that nano-silver particles of 30 to 40 nm in size were homogeneously dispersed in the solution. The possible mechanism of D-CTS on the reduction and stabilization of AgNPs may be due to the formation of four-coordinate complexes. The synthesized AgNPs remained stable for more than three months.

*Keywords:* Dialdehyde chitosan; Silver nanoparticles; Green synthesis; Polysaccharide

*Contact information:* a: Key laboratory of Eco-textile, Ministry of Education, Jiangnan University, Wuxi, 214122, China; b: School of Engineering and Information of Yiwu Industrial & Commercial College, Yiwu, 322000, China; \*Corresponding author: longzhu@jiangnan.edu.cn

### INTRODUCTION

The preparation of metal nanoparticles is a major research area in nanoscience and engineering, given their unusual chemical and physical properties such as catalytic activity, novel electronic, optic and magnetic properties, as well as application potential in biotechnology. A variety of methodologies have been reported for the preparation of metallic nanoparticles (Pal *et al.* 2009), among which notable examples include salt reduction (Fan *et al.* 2008; Pillai and Kamat 2004), thermal reduction with starch (Vigneshwaran *et al.* 2006), irradiation (Kassaei *et al.* 2008), and electrochemical synthesis (Starowicz *et al.* 2006; Zhu *et al.* 2001). To date, most reported synthetic methods for the preparation of silver nanoparticles rely heavily on the use of organic solvents and toxic reducing agents such as hydrazine (Sakai *et al.* 2006), N,N-dimethylformamide (Pastoriza-Santos and Liz-Marzán 2002), and sodium borohydride (Van Hying *et al.* 2001). All these chemicals are highly reactive and pose potential environmental and biological risks.

The increasing awareness regarding green chemistry has prompted interest in an eco-friendly approach to synthesize nanoparticles that is simple, cost-effective, compatible with biomedical and pharmaceutical applications, and scalable for commercial production (Travan *et al.* 2009). The development of green chemistry

approaches is desirable in order to reduce waste and pursue sustainability. A green method for nanoparticle preparation should be evaluated from three aspects: the solvent, the reducing agent, and the stabilizing agent. Earlier reports have investigated the use of natural polymers including chitosan (Huang *et al.* 2004), heparin (Guo and Yan 2008), and soluble starch (Yoksan and Chirachanchai 2010) as reducing and stabilizing agents for the preparation of silver nanoparticles.

Chitosan is one of the most abundant materials that is easily obtained in nature (Fan *et al.* 2011; Rani *et al.* 2010). It is particularly interesting in metal nanoparticle synthesis due to its interactions with metal ions and metal nanoparticles. The metal ions can be evenly dispersed throughout the chitosan polymer by chelation (Travan *et al.* 2009). However, chitosan is soluble in water only at low pH as a polycation, which is a serious limitation. Besides, it is immiscible with other oppositely charged polyelectrolytes and requires the addition of another reducing agent in the reaction (Bae 2010; Fan *et al.* 2011; Zhou *et al.* 2012). To overcome these problems, a new method was developed to prepare silver nanoparticles using Dialdehyde Chitosan (D-CTS). D-CTS is generated by the periodate oxidization of chitosan and its solubility is no longer restricted by the pH value of the solution. In addition, the dialdehyde groups in D-CTS can act both as a reducing agent and as a stabilizing agent, hence eliminating the need for adding external reducing agent during the nanoparticle synthesis. It has been proposed that the higher sorption capacity of D-CTS is due to its increased chain flexibility and higher concentrations of chelating groups. Specifically, the amino groups and the aldehyde groups can coordinate to the metal ions to form a polymer–metal complex, which can then be reduced under mild conditions to generate metal nanoparticles with a smaller size and a narrower size distribution.

## EXPERIMENTAL

### Materials and Methods

Chitosan, silver nitrate, sodium periodate, and all other reagents were of analytical grade and used without further purification. Chitosan has a deacetylation degree of  $\geq 91\%$  and a molecular weight ( $M_w$ ) of 235 kDa (determined by the viscosity method). Distilled water was used as the solvent in all experiments.

### Preparation and Characterization of Dialdehyde Chitosan (D-CTS)

Dialdehyde Chitosan (D-CTS) was prepared by a modified method of Vold *et al.* (Vold and Christensen 2005), as schematically shown in Fig. 1. Chitosan (2.0 g, containing about 12 mmol GlcN monomer) was dissolved in acetate buffer (160 mL, pH = 3.0) overnight, and the obtained clear solution was degassed by purging N<sub>2</sub> for 30 min. The sodium periodate solution of different concentrations (IO<sub>4</sub><sup>-</sup>/chitosan molar ratio at 0.1, 0.5, 0.75, and 1 for different experiments) was then slowly added to the chitosan solution under magnetic stirring and the mixture was maintained at 4 °C for 48 h, before dialyzing (Spectra/Por membrane, MWCO = 3500) against NaCl (0.2 M, pH = 3.0 using hydrochloric acid) for 3 d and against deionized water (pH = 3.0 using hydrochloric acid) for 5 d. The dialysate was passed through a syringe filter (0.22 μm) and lyophilized.

## Preparation of Silver Nanoparticles (AgNPs) Using D-CTS

An aqueous solution of  $\text{AgNO}_3$  (1 mL,  $1 \times 10^{-3}$  M) was added to an aqueous solution of D-CTS (2 mL,  $1 \times 10^{-3}$  M) with different dialdehyde content (shown in Table 1). The final pH was adjusted to 2, 3, 4, 5, and 6, respectively, using nitric acid. The reaction mixture was maintained in a 70 °C water bath under magnetic stirring for 6 h for the reaction to complete. The solution was initially colorless and turned yellow, indicating the formation of AgNPs. Finally, the AgNPs solutions were centrifuged at 10,000 rpm for 30 min and the residue was lyophilized.

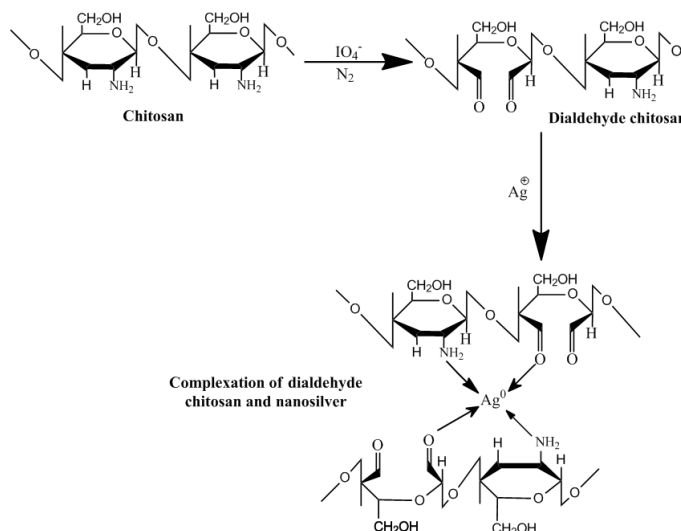


Fig. 1. The synthesis of AgNPs

## Characterization of D-CTS

The FT-IR spectra of periodate-oxidized chitosan were recorded on a Perkin-Elmer FT-IR spectrometer (Spectrum GX). The  $^1\text{H-NMR}$  spectra were recorded on an Avance 600 (Bruker, Germany) spectrometer operating at 400 MHz. Elemental analysis (C, N) was performed on a Perkin-Elmer 2400 Series II Analyzer. Before elemental analysis, the polymer samples were thoroughly dried by lyophilization for 3 days. Elemental analysis should directly reflect the relative dialdehyde content ( $F_{\text{ox}}$ ) according to the following equation (Jiang *et al.* 2011; Ping *et al.* 2011),

$$\frac{\text{N}}{\text{C}} = \frac{F_A + (1 - F_A) \cdot (1 - F_{\text{ox}})}{2 F_A + 6} \quad (1)$$

where  $F_A$  is the content of acetylated units in the molecular chain of chitosan.

## Characterization of Silver Nanoparticles

### UV-Visible spectral analysis

A color change of the reaction mixture can clearly indicate the formation of AgNPs. Therefore, the absorbance was measured using a double beam UV-Visible spectrophotometer (Cary 100, Varian) at a resolution of 1 nm over the range of 190 to 650 nm.

### Dynamic light scattering (DLS)

The size distribution and the average size of the synthesized AgNPs were determined by dynamic light scattering (DLS). DLS (Malvern, UK) measurements were carried out for the size range from 0.1 nm to 10  $\mu\text{m}$ .

### Fourier-transform infrared spectroscopy (FT-IR)

The characterization of functional groups on the surface of AgNPs was performed by Fourier-transform infrared spectroscopy (FT-IR) (Perkin-Elmer, Germany). The spectra were scanned over 500 to 4000  $\text{cm}^{-1}$  at a resolution of 4  $\text{cm}^{-1}$ .

### X-ray diffraction (XRD)

X-ray diffraction measurements were carried out on a Philips PW-1730 system operating at the Co  $K\alpha$  wavelength of 1.7889  $\text{\AA}$ , 30 mA, and 40 kV.

### Scanning electron microscope (SEM)

The surface and the morphology of the AgNPs were examined under a scanning electron microscope (Hitachi S-4800, Japan).

## RESULTS AND DISCUSSION

### Effect of the $\text{GlcN}/\text{IO}_4^-$ Molar Ratio on the Oxidation Degree of Chitosan

The periodate oxidation of diols is a widely employed routine method for elucidating structures of carbohydrates or polysaccharides including cellulose, starch, glycogen, and xylan. During this oxidation reaction, the periodate ion splits the carbon-carbon bond of vicinal diols to form dialdehyde.

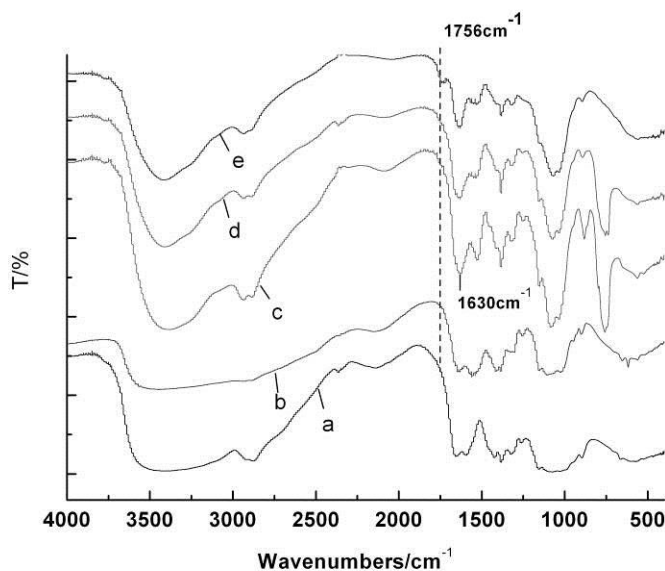


**Fig. 2.** FT-IR spectra of D-CTS prepared by using different  $\text{GlcN}/\text{IO}_4^-$  molar ratios. (a: chitosan, b: D-CTS,  $\text{GlcN}/\text{IO}_4^- = 1:0.1$ , c: D-CTS,  $\text{GlcN}/\text{IO}_4^- = 1:0.5$ , d: D-CTS,  $\text{GlcN}/\text{IO}_4^- = 1:0.75$ , e: D-CTS,  $\text{GlcN}/\text{IO}_4^- = 1:1$ )

The absorption at  $1756\text{ cm}^{-1}$  in the FT-IR spectra is characteristic of the aldehyde groups that resulted from the periodate mediated oxidation (Wang *et al.* 2010). In addition, the intensity of this peak increases with rising GlcN/ $\text{IO}_4^-$  molar ratio (shown in Fig. 2), indicating the formation of more aldehyde groups when using more periodate.

Figure 3 shows the  $^1\text{H-NMR}$  spectra of chitosan before and after oxidation. It can be observed that the signals at 3.0 to 3.1 ppm (due to the proton on C-2 of GlcN) were significantly attenuated for the D-CTS, indicating the oxidative cleavage of the C–C bond and the formation of the dialdehyde units. The oxidation degree of chitosan was quantified based on both  $^1\text{H-NMR}$  and elemental analysis (Jia *et al.* 2011), and the results were in good agreement (Table 1).

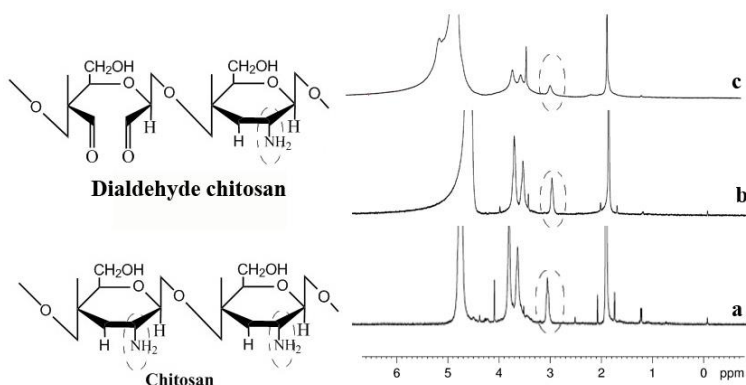


**Fig. 3.**  $^1\text{H-NMR}$  spectra of chitosan before and after oxidation. (a: chitosan, b: D-CTS, GlcN/ $\text{IO}_4^-$  = 1:0.5, c: D-CTS, GlcN/ $\text{IO}_4^-$  = 1:1)

**Table 1.** Dialdehyde Content and Molecular Weight of Oxidized Chitosan

Polymer	GlcN/ $\text{IO}_4^-$ Molar Ratio	Degree of Oxidation *		$M_w$ (KDa)
		$^1\text{H-NMR}$	Elemental Analysis	
D-CTS-1	0.1	$5.1 \pm 1.3$	$4.5 \pm 0.6$	45.7
D-CTS-2	0.5	$18.1 \pm 0.9$	$19.4 \pm 0.4$	25.7
D-CTS-3	0.75	$32.3 \pm 0.9$	$31.3 \pm 0.3$	15.6
D-CTS-4	1.0	$48.6 \pm 0.7$	$46.3 \pm 0.4$	13.1

\* The degree of oxidation is expressed as the percentage of dialdehyde groups per 100 GlcN units.  $M_w$  was determined by the viscosity method.

### UV-Vis Absorption Spectrum of D-CTS Capped AgNPs

#### *Influence of the oxidation degree of D-CTS on the synthesis and stability of AgNPs*

Silver nanoparticles absorb radiation in the visible region of the electromagnetic spectrum (*ca.* 380 to 450 nm) due to the excitation of surface plasmon vibrations; this effect is responsible for the striking yellow-brown color of silver nanoparticles in various media (Khanna and Subbarao 2003; Sakai *et al.* 2006). The UV–Vis absorption spectra of the silver nanoparticle solutions are shown in Fig. 4. The plasmon absorbance of the silver nanoparticles was observed at 416 nm, and the plasmon band was symmetric,

indicating that the solution did not contain many aggregated particles. This is in agreement with the scanning electron micrograph observations.

Silver nanoparticles were obtained by using D-CTS as both the reducing agent and the stabilizing agent. The reducing and chelating properties of D-CTS make it possible to prepare silver nanoparticles by using this polysaccharide as both the reducing agent and the stabilizing agent. The abundance of aldehyde groups in D-CTS enriched the  $\text{Ag}^+$  ions in the solution, thus facilitating the formation of silver nanoparticles. The UV–Vis spectra of different silver nanoparticles are shown in Fig. 4(A). When the degree of oxidation of D-CTS was 32.3%, the stabilization and reduction of  $\text{Ag}^+$  ions was optimal and the maximum peak absorbance was obtained.

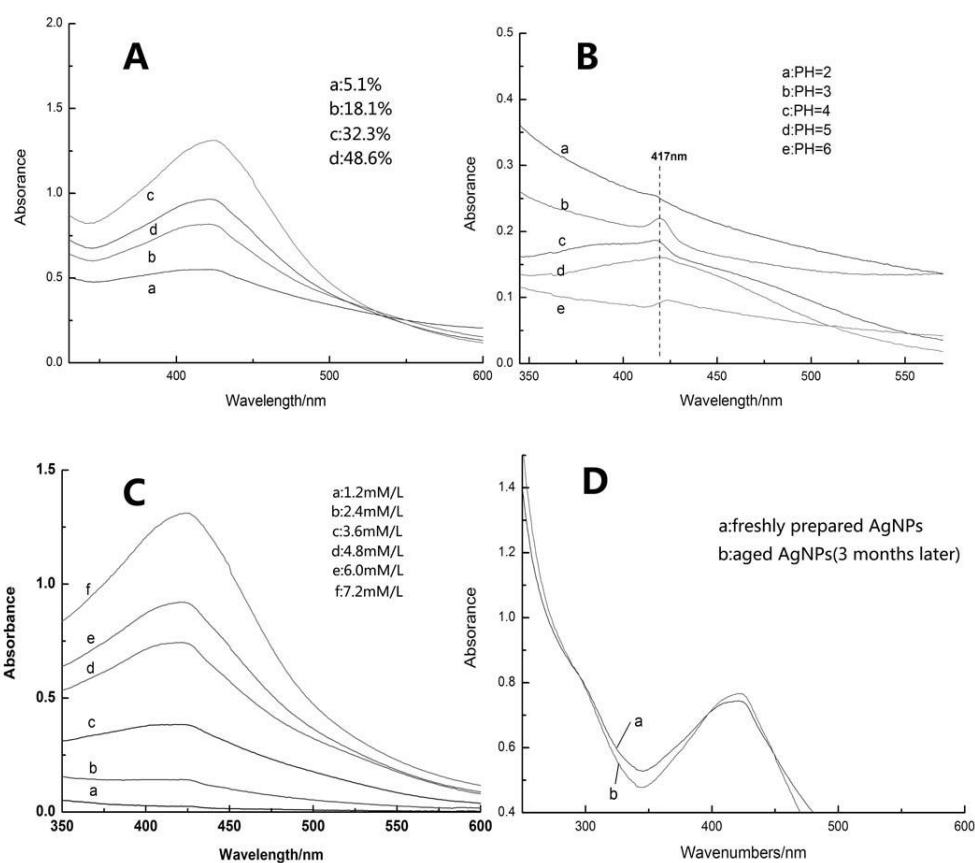


**Fig. 4.** Effect on UV–vis spectra of silver nanoparticles prepared using D-CTS of (A) different dialdehyde contents at PH = 3, (B) different pH, (C) different concentrations of D-CTS, and (D) different stored time

#### *Influence of the solution pH on the synthesis and stability of AgNPs*

D-CTS contains four major classes of functional groups, including the hydroxyl group ( $-\text{OH}$ ), the amine group ( $-\text{NH}_2$ ), the aldehyde group ( $-\text{CHO}$ ), and the carboxylate ( $-\text{COO}^-$ ) group, and it is sensitive to variations in the pH value of the aqueous medium. Therefore, the formation of AgNPs as a function of the pH value of the medium was analyzed, as shown in Fig. 4(B).

The spectra exhibited an absorption band at around 417 nm, which is the characteristic Surface Plasmon Resonance (SPR) band of AgNPs and confirms the formation of AgNPs. The intensity of the SPR band of AgNPs increased significantly

when the pH was increased from 2 to 3 and attained maximum intensity at pH 3 to 4, but then began to decrease when the pH was further increased to 6. This is possibly because at pH below 3, the amino groups become protonated and are thus unable to stabilize the  $\text{Ag}^+$  ions. On the other hand, at pH above 4, the formation of intra- and intermolecular Schiff base will be unfavorable for the formation of AgNPs. Hence, the pH value of 3 was selected as the optimum pH for the synthesis of AgNPs.

#### *Influence of the concentration of D-CTS on the synthesis and stability of AgNPs*

The stoichiometry of the complexes were determined using Job's method of continuous variation and the molar ratio method (Pillai and Kamat 2004). The structure of the complexes could be evaluated by the optimum molar ratio of metal ions and ligand. The  $\text{Ag}^+$  concentration was kept constant at  $2.4 \times 10^{-3}$  mol/L while the D-CTS concentration was increased in regular steps ( $1.2, 2.4, 3.6, 4.8 \dots \times 10^{-3}$  mol/L). Figure 4(C) shows the maximum absorption at  $C_{\text{Glacn}}/C_{\text{Ag}}$  equal to 3:1 (*i.e.*,  $7.2/2.4$ ). Based on the dialdehyde content of D-CTS-3, the  $C_{\text{aldehyde}}/C_{\text{Ag}}$  ratio was equal to 2:1 (*i.e.*,  $4.65 \times 10^{-3}$  mol/L to  $2.4 \times 10^{-3}$  mol/L). In addition,  $C_{\text{NH}_2}/C_{\text{Ag}} = 2:1$ . Both results indicate a 2:1 complex. It is generally known that the coordination of amino acid to silver ion seems to occur through the amino group or the carboxyl group, forming two- or four-coordinate complexes. Based on the results, the D-CTS silver complex may be a four-coordinate complex (as shown in Fig. 1).

#### *Evaluation the stability of the AgNPs synthesized by D-CTS*

The stability of the synthesized AgNPs was assessed by measuring absorbance intensities of the freshly prepared AgNPs and the aged AgNPs. Figure 4(D) shows no significant change in the absorbance intensity and wavelength of the AgNPs after storage for 3 months at room temperature. This observation rules out particle agglomeration and verifies the excellent stability of the AgNPs solution.

### Particle Size Analysis of AgNPs

The average particle size and the size distribution of the synthesized AgNPs were determined by DLS, and the results are shown in Fig. 5.

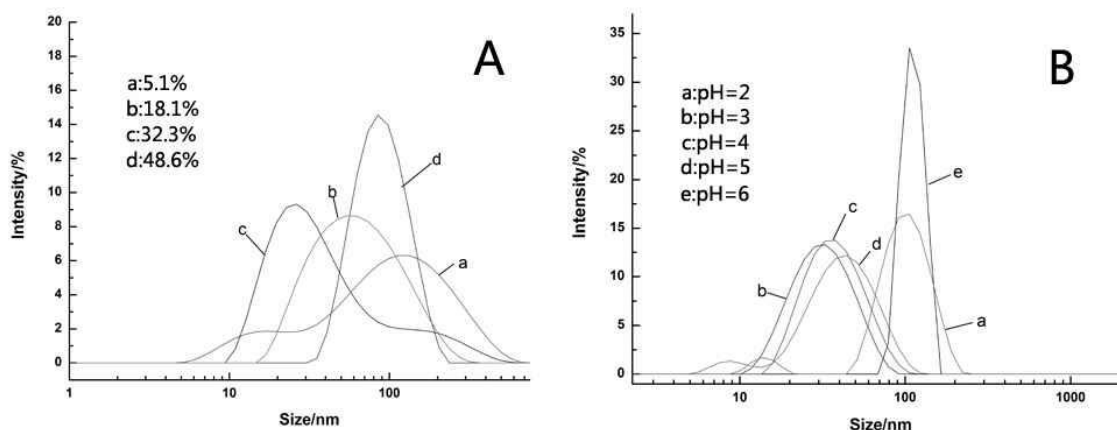


**Fig. 5.** DLS analysis of AgNPs prepared (A) using D-CTS with different dialdehyde contents at pH = 3, (B) using D-CTS-3 at different pH

As indicated, the average size of the prepared AgNPs was about 20 to 30 nm. By comparison, it can also be noted that using D-CTS with 32.3% dialdehyde content at pH = 3 produced the smallest AgNPs with highest monodispersity. These results are in agreement with the UV-Visible spectroscopy results.

### FT-IR Spectrum Studies of D-CTS Capped AgNPs

As shown in Fig. 6, the FT-IR spectrum of the synthesized AgNPs exhibited absorption bands of O–H stretching at  $3423.07\text{ cm}^{-1}$ , C–H stretching at  $2918.18\text{ cm}^{-1}$ , C=O stretching at  $1750.20\text{ cm}^{-1}$ , and N–H stretching of primary amines at  $1627.14\text{ cm}^{-1}$ , respectively. The C–N absorption at  $1350\text{ to }1390\text{ cm}^{-1}$  overlapped with the absorption of residual  $\text{NO}_3^-$ , and the weak broad band at  $990\text{ to }1100\text{ cm}^{-1}$  may represent the bending vibrations of C–OH in chitosan (Annadhasan *et al.* 2012). Thus the C=O and the N–H groups have a stronger ability to bind with the metal and may perform dual functions in the formation and stabilization of the AgNPs.

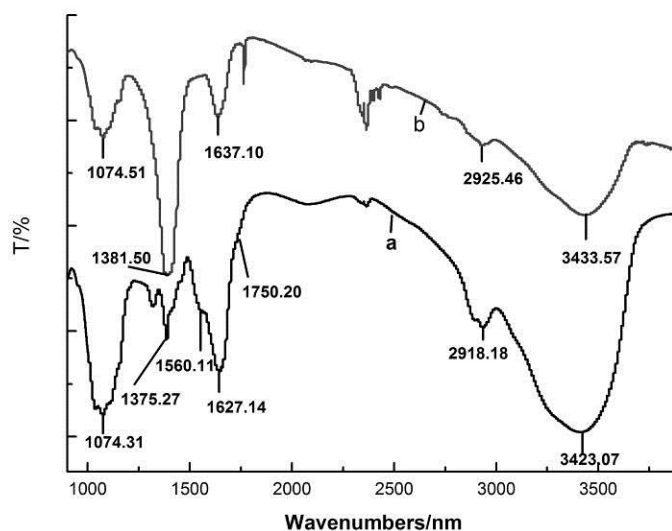


**Fig. 6.** Typical FT-IR spectra of (a) D-CTS and (b) D-CTS capped AgNPs

The absorption peaks at  $1750.20$ ,  $1627.14$ , and  $1560.11\text{ cm}^{-1}$  correspond to the stretching mode of C=O and N–H groups in D-CTS, which are merged into a single peak at  $1637.10\text{ cm}^{-1}$  after reaction with  $\text{Ag}^+$ . This may be due to the non-bonding lone pair electrons of the C=O and the nitrogen that interacted with the AgNPs.

### X-ray Diffraction (XRD) of D-CTS Capped AgNPs

The XRD patterns of chitosan (CTS), D-CTS, and AgNPs are shown in Fig. 7. The strong crystalline diffraction peaks of CTS at  $20.1^\circ$  and  $11.2^\circ$  disappeared after the oxidization reaction, indicating that the crystalline structure of CTS was completely destroyed during the oxidization reaction and an amorphous structure was formed. The synthesized AgNPs (Fig. 7 (c)) have peaks with  $2\theta$  values of  $37.45^\circ$  and  $44.47^\circ$ , which can be assigned to the (111) and (200) reflection planes of face-centered cubic (FCC) silver (Kassaei *et al.* 2008; Vasileva *et al.* 2011).

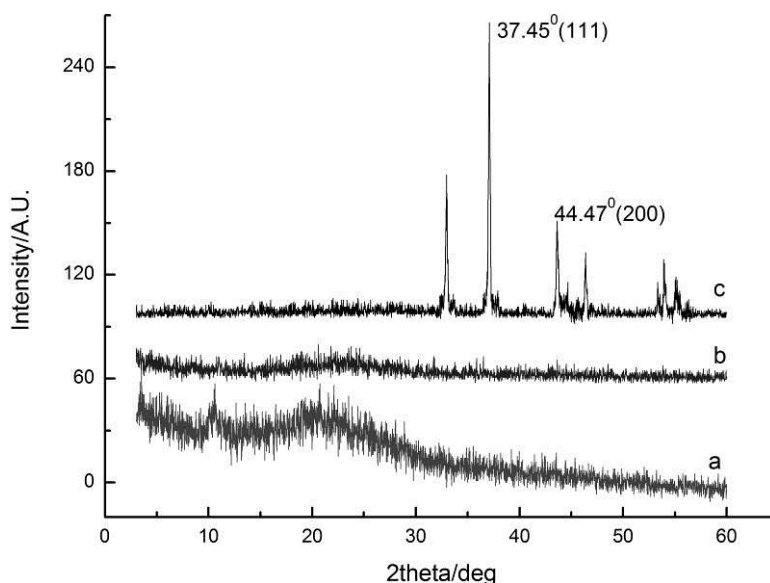


**Fig. 7.** XRD patterns of (a) CTS, (b) D-CTS, (c) D-CTS capped AgNPs

### Scanning Electron Microscopy (SEM) of D-CTS Capped AgNPs

As the SEM images in Fig. 8 show, the shape of the prepared AgNPs was predominantly spherical. No block flocculation was observed, indicating the absence of the accumulation of silver particles and that D-CTS had good stabilizing effect for the AgNPs. The size of the prepared AgNPs was about 30 to 40 nm. These results are in agreement with the DLS analysis.

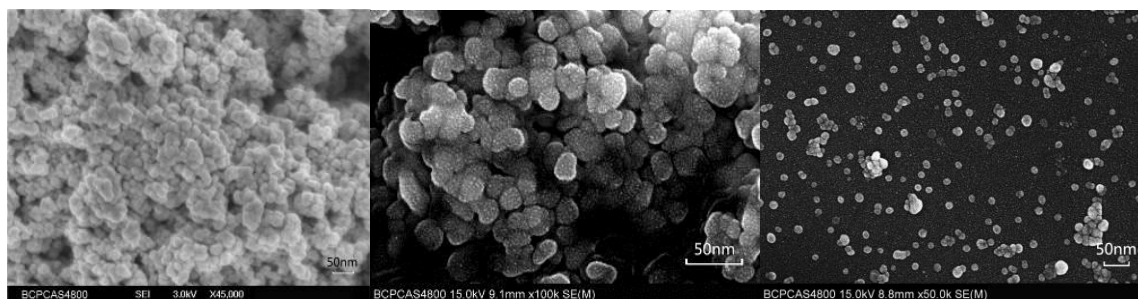


**Fig. 8.** SEM images of AgNPs prepared using D-CTS with different magnification. (7.2 mM/mL D-CTS + 2.4mM AgNO<sub>3</sub> at pH = 3; the dialdehyde contents of D-CTS was 32.3%.)

## CONCLUSIONS

1. The present study describes a green method to synthesize silver nanoparticles AgNPs in the presence of dialdehyde chitosan (D-CTS) in aqueous medium. It was observed that D-CTS acted both as the reducing agent and as the stabilizing agent. The aldehyde groups of D-CTS were involved in the reduction of the Ag<sup>+</sup> ions, while the amine groups bound strongly to the surface of the nanoparticles (NPs).

2. UV–Visible, DLS, and SEM measurements were carried out to characterize the resulting silver nanoparticles (AgNPs). The morphology and size distribution of AgNPs varied with the dialdehyde contents of D-CTS and the pH values of the reaction solution.
3. The X-ray diffraction (XRD) spectrum of the prepared AgNPs showed high crystallinity and face-centered cubic structure of the nanoparticles. The FT-IR spectra demonstrated that the functional groups present in the prepared AgNPs include aldehyde groups and amino groups. The possible mechanism of D-CTS on the reduction and stabilization of AgNPs may be due to the formation of four coordinate complexes. This approach for AgNPs synthesis is safer for use in biological and biomedical applications.

## ACKNOWLEDGMENTS

This research was financially supported by the National Nature Science Foundation of China (No. 31270633) and the collegiate program of Yiwu Industrial & Commercial College (No. 2013029)

## REFERENCES CITED

- Annadhasan, M., SankarBabu, V. R., Naresh, R., Umamaheswari, K., and Rajendiran, N. (2012). "A sunlight-induced rapid synthesis of silver nanoparticles using sodium salt of N-cholyl amino acids and its antimicrobial applications," *Colloids and Surfaces B: Biointerfaces* 96, 14-21.
- Bae, H.-S. (2010). "Functional modification of sanitary nonwoven fabric by chitosan/nanosilver colloid solution and evaluation of applicability," *Fibers and Polymers* 11(4), 606-614.
- Fan, F.-R., Liu, D.-Y., Wu, Y.-F., Duan, S., Xie, Z.-X., Jiang, Z.-Y., and Tian, Z.-Q. (2008). "Epitaxial growth of heterogeneous metal nanocrystals: From gold nanooctahedra to palladium and silver nanocubes," *Journal of the American Chemical Society* 130(22), 6949-6951.
- Fan, L.-H., Pan, X.-R., Zhou, Y., Chen, L.-Y., Xie, W.-G., Long, Z.-H., and Zheng, H. (2011). "Preparation and characterization of crosslinked carboxymethyl chitosan-oxidized sodium alginate hydrogels," *Journal of Applied Polymer Science* 122(4), 2331-2337.
- Guo, Y., and Yan, H. (2008). "Preparation and characterization of heparin - stabilized gold nanoparticles," *Journal of Carbohydrate Chemistry* 27(5), 309-319.
- Huang, H., Yuan, Q., and Yang, X. (2004). "Preparation and characterization of metal-chitosan nanocomposites," *Colloids and Surfaces B: Biointerfaces* 39(1–2), 31-37.
- Jia, Y., Hu, Y., Zhu, Y., Che, L., Shen, Q., Zhang, J., and Li, X. (2011). "Oligoamines conjugated chitosan derivatives: Synthesis, characterization, in vitro and in vivo biocompatibility evaluations," *Carbohydrate Polymers* 83(3), 1153-1161.
- Jiang, H.-L., Lim, H.-T., Kim, Y.-K., Arote, R., Shin, J.-Y., Kwon, J.-T., Kim, J.-E., Kim, J.-H., Kim, D., Chae, C., Nah, J.-W., Choi, Y.-J., Cho, C.-S., and Cho, M.-H.

- (2011). "Chitosan-graft-spermine as a gene carrier in vitro and in vivo," *European Journal of Pharmaceutics and Biopharmaceutics* 77(1), 36-42.
- Kassae, M. Z., Akhavan, A., Sheikh, N., and Beteshobabrud, R. (2008). "γ-Ray synthesis of starch-stabilized silver nanoparticles with antibacterial activities," *Radiation Physics and Chemistry* 77(9), 1074-1078.
- Khanna, P. K., and Subbarao, V. (2003). "Nanosized silver powder via reduction of silver nitrate by sodium formaldehydesulfoxylate in acidic pH medium," *Materials Letters* 57(15), 2242-2245.
- Pal, A., Shah, S., and Devi, S. (2009). "Microwave-assisted synthesis of silver nanoparticles using ethanol as a reducing agent," *Materials Chemistry and Physics* 114(2-3), 530-532.
- Pastoriza-Santos, I., and Liz-Marzán, L. M. (2002). "Synthesis of silver nanoprisms in DMF," *Nano Letters* 2(8), 903-905.
- Pillai, Z. S., and Kamat, P. V. (2004). "What factors control the size and shape of silver nanoparticles in the citrate ion reduction method?" *Journal of Physical Chemistry B* 108(3), 945-951.
- Ping, Y., Liu, C. D., Zhang, Z. X., Liu, K. L., Chen, J. H., and Li, J. (2011). "Chitosan-graft-(PEI-beta-cyclodextrin) copolymers and their supramolecular PEGylation for DNA and siRNA delivery," *Biomaterials* 32(32), 8328-8341.
- Rani, M., Agarwal, A., and Negi, Y. S. (2010). "Review: Chitosan based hydrogel polymeric beads—as drug delivery system," *BioResources* 5(4), 2765-2807.
- Sakai, H., Kanda, T., Shibata, H., Ohkubo, T., and Abe, M. (2006). "Preparation of highly dispersed core/shell-type titania nanocapsules containing a single Ag nanoparticle," *Journal of the American Chemical Society* 128(15), 4944-4945.
- Starowicz, M., Stypuła, B., and Banaś, J. (2006). "Electrochemical synthesis of silver nanoparticles," *Electrochemistry Communications* 8(2), 227-230.
- Travan, A., Pelillo, C., Donati, I., Marsich, E., Benincasa, M., Scarpa, T., Semeraro, S., Turco, G., Gennaro, R., and Paoletti, S. (2009). "Non-cytotoxic silver nanoparticle-polysaccharide nanocomposites with antimicrobial activity," *Biomacromolecules* 10(6), 1429-1435.
- Van Hying, D. L., Klemperer, W. G., and Zukoski, C. F. (2001). "Silver nanoparticle formation: Predictions and verification of the aggregative growth model," *Langmuir* 17(11), 3128-3135.
- Vasileva, P., Donkova, B., Karadjova, I., and Dushkin, C. (2011). "Synthesis of starch-stabilized silver nanoparticles and their application as a surface plasmon resonance-based sensor of hydrogen peroxide," *Colloids and Surfaces A: Physicochemical and Engineering Aspects* 382(1-3), 203-210.
- Vigneshwaran, N., Nachane, R. P., Balasubramanya, R. H., and Varadarajan, P. V. (2006). "A novel one-pot 'green' synthesis of stable silver nanoparticles using soluble starch," *Carbohydrate Research* 341(12), 2012-2018.
- Vold, I. M. N., and Christensen, B. E. (2005). "Periodate oxidation of chitosans with different chemical compositions," *Carbohydrate Research* 340(4), 679-684.
- Wang, X., Yao, J., Zhou, J. P., Lu, Y., and Wang, W. (2010). "Synthesis and evaluation of chitosan-graft-polyethylenimine as a gene vector," *Pharmazie* 65(8), 572-579.
- Yoksan, R., and Chirachanchai, S. (2010). "Silver nanoparticle-loaded chitosan–starch based films: Fabrication and evaluation of tensile, barrier and antimicrobial properties," *Materials Science and Engineering: C* 30(6), 891-897.

Zhou, Y., Zhao, Y., Wang, L., Xu, L., Zhai, M., and Wei, S. (2012). "Radiation synthesis and characterization of nanosilver/gelatin/carboxymethyl chitosan hydrogel," *Radiation Physics and Chemistry* 81(5), 553-560.

Zhu, J.-J., Liao, X.-H., Zhao, X.-N., and Chen, H.-Y. (2001). "Preparation of silver nanorods by electrochemical methods," *Materials Letters* 49(2), 91-95.

Article submitted: March 27, 2013; Peer review completed: July 18, 2013; Revised version accepted: October 11, 2013; Published: October 14, 2013.